Spectroscopy of ^{23}Al and ^{27}P using the (^{7}Li,^{8}He) reaction and the implications for ^{22}Na and ^{26}Al nucleosynthesis in explosive hydrogen burning

J. A. Caggiano,[1,*] D. Bazin,[1] W. Benenson,[1] B. Davids,[1] R. Ibbotson,[1,†] H. Scheit,[1,‡] B. M. Sherrill,[1] M. Steiner,[1] J. Yurkon,[1] A. F. Zeller,[1] B. Blank,[2] M. Chartier,[1,5,§] J. Greene,[3] J. A. Nolen, Jr.,[3] A. H. Wuosmaa,[3] M. Bhattacharya,[4] A. Garcia,[4] and M. Wiescher[4]

[1]*National Superconducting Cyclotron Laboratory, Michigan State University, East Lansing, Michigan 48824*

[2]*Centre d'Etudes Nucléaires de Bordeaux-Gradignan, F-33175 Gradignan Cedex, France*

[3]*Argonne National Laboratory, Argonne, Illinois 60439*

[4]*University of Notre Dame, Notre Dame, Indiana 46556*

[5]*Oak Ridge National Laboratory, P. O. Box 2008, Oak Ridge, Tennessee 37831-368*

(Received 11 July 2000; published 29 June 2001)

The proton-rich nuclei ^{23}Al and ^{27}P were studied using the ^{24}Mg(^{7}Li,^{8}He)^{23}Al and ^{28}Si(^{7}Li,^{8}He)^{27}P reactions, respectively. Several energy levels are observed in each nucleus. The mass excess of ^{23}Al was measured to be 6.773(28) MeV and the mass excess of ^{27}P was measured to be $-0.670(41)$ MeV. The first excited state of ^{23}Al has been resolved from the ground state for the first time at an excitation energy of $E_x = 0.550(20)$ MeV. The first excited state of ^{27}P has been measured for the first time at an excitation energy of $E_x = 1.199(19)$ MeV. The astrophysical implications of these results for the reaction rates of ^{22}Mg$(p,\gamma)^{23}$Al and ^{26}Si$(p,\gamma)^{27}$P for the nucleosynthesis of ^{22}Na and ^{26}Al in Ne novae will be discussed.

DOI: 10.1103/PhysRevC.64.025802 PACS number(s): 25.70.Hi, 27.30.+t, 26.30.+k

I. MOTIVATION

The ability to detect γ rays from astrophysical sources with space-based telescopes has increased interest in understanding nucleosynthesis in novae, especially the synthesis of the γ-ray emitters themselves. These observed γ rays can be used to constrain existing nova models. While the dynamics of the astrophysical event dominate the uncertainties that go into the model calculations, the nuclear database also contributes substantial uncertainty in the model predictions. The most important reactions to study must be identified, and it is imperative to study the nuclei involved in those reactions. The production of two of these γ-ray emitters ^{22}Na and ^{26}Al, may depend substantially on the structures and masses of ^{23}Al and ^{27}P, respectively, yet the structures of these two nuclei are mostly unknown. Little is known about the resonances just above the proton threshold, and the masses of the two nuclei are only known with $\approx$30 keV accuracy. The goal of this experiment was to identify excited states of ^{23}Al and ^{27}P just above the proton threshold and to measure their masses with the high-resolution S800 spectrograph at MSU.

II. BACKGROUND

Explosive hydrogen burning is triggered by thermonuclear runaways in electron degenerate hot and dense stellar environments. Novae [1] have been identified by light curve and luminosity observations as possible sites for such events. Novae are initiated by accretion processes in close binary systems. Material from a massive main sequence or red giant star overflows from the Roche-Lobe and accretes on the surface of a highly electron degenerate white dwarf. Mixing between the white dwarf material and the accreted envelope causes enrichment of the accreted material in C and O for the case of a CO white dwarf, or in O, Ne, and possibly Mg for the case of an ONeMg white dwarf, respectively. After a critical mass has been accreted a thermonuclear runaway is triggered by the energy release from the pp chains and the hot CNO cycles at typical densities between 10^2 and 10^3 g/cm^3. Peak temperatures of up to 0.4 GK can be reached before degeneracy is lifted. A typical temperature and density curve is shown in Fig. 1 [2]. The energy release from the thermonuclear runaway and subsequently from the decay of the freshly produced radioisotopes ^{15}O, ^{17}F, and ^{18}F dominate the luminosity curve. The associated photon pressure and the gas pressure cause rapid expansion and eventually ejection of the accreted envelope. Observations of strong Ne lines in some nova [3] (Ne nova) have been classified as thermonuclear runaways on ONeMg white dwarfs with initial Ne enrichment. While the energy generation is still predominantly driven by the hot CNO cycles, substantial nucleosynthesis in the Ne to S range can take place via the NeNa and the MgAl cycles [4]. This fact has been confirmed by the recent observation of high Si, P, and S abundances in Ne novae [1,5]. Detailed model calculations have been performed for nucleosynthesis in Ne novae [2,6,7] which indicated considerable discrepancies in the abundance predictions for the ejecta. These discrepancies are partly due to differences in the adopted abundance distribution of the white dwarf material but also due to differences in hydrodynamical and nuclear physics-related model parameters. Two-

*Present address: Argonne National Laboratory, Argonne, IL 60439.

†Present address: Brookhaven National Laboratory, Upton, NY 11973-5000.

‡Present address: Max-Planck-Institut für Kernphysik, Heidelberg, Germany.

§Present address: Centre d'Etudes Nucléaires de Bordeaux-Gradignan, F-33175 Gradignan Cedex, France.

and three-dimensional studies clearly indicate that the hydrodynamical and convective processes prior to and during the thermonuclear runaway are still far from being understood [1,8,9] and the respective treatment may cause substantial differences in the model predictions. The predictions however also show considerable discrepancies with the observed abundance distributions in the ejecta. These discrepancies may be partly due to the difficulties associated with the spectral analysis which depends on a correct model treatment of the expanding novae atmosphere and its condensation and opacity [10]. This situation, however, should little affect the observation of long-lived radioactive isotopes such as ^{22}Na and ^{26}Al which are predicted to be abundantly produced in novae nucleosynthesis [2]. Observations with satellite γ telescopes such as COMPTEL of the characteristic ^{22}Na ($E_\gamma = 1.275$ MeV) and ^{26}Al ($E_\gamma = 1.86$ MeV) activities only yielded upper limits, which in the case of ^{22}Na was substantially below the predicted abundance [11]. While this discrepancy again may be explained by the insufficiency of the theoretical models, there are still considerable uncertainties with respect to the nuclear physics aspects of the nucleosynthesis in the Ne-S range [12–14].

In novae, ^{22}Na is produced during the thermonuclear runaway and the high-temperature phase via the reaction sequence ^{20}Ne$(p,\gamma)^{21}$Na$(p,\gamma)^{22}$Mg$(\beta^+\nu)^{22}$Na but is depleted by the ^{22}Na(p,γ) process [15,16]. The predicted ^{22}Na equilibrium abundance, however, might be substantially reduced by a strong ^{22}Mg$(p,\gamma)^{23}$Al reaction with a subsequent ^{23}Al(p,γ) process, effectively by-passing the production of ^{22}Na. This process depends directly on the reaction rates of both capture processes ^{22}Mg$(p,\gamma)^{23}$Al and ^{23}Al$(p,\gamma)^{24}$Si which are determined by direct capture and low-energy resonance contributions. Whether the ^{22}Mg beta decays to ^{22}Na or undergoes the two-step proton capture to ^{24}Si is uncertain for a wide range of burning conditions due to the large uncertainties in the mass (± 25 keV) and first excited state energy (± 60 keV) of ^{23}Al. A direct measurement of the reaction cross sections would require intense radioactive ^{22}Mg and ^{23}Al beams. Since such beams are not available yet, the present rates are based on an indirect study of the level structure of the respective compound nuclei ^{23}Al [17] and ^{24}Si [14]. The only previous measurement of the level structure of ^{23}Al was performed via the ^{24}Mg(^{7}Li,^{8}He) reaction but carries considerable uncertainties. Due to limited experimental resolution, the excitation energy of the first excited state is not well known. This translates directly into more than an order of magnitude uncertainty in the reaction rate. Improved energy resolution would reduce the uncertainty considerably and would put the present reaction rate on much firmer experimental ground.

Satellite based γ telescope observation indicate an intense ^{26}Al distribution throughout the galactic plane [18]. The origin of ^{26}Al is still under debate but one potential source is nova induced nucleosynthesis [1]. The production of ^{26}Al in novae is dominated by the reaction sequence ^{24}Mg$(p,\gamma)^{25}$Al$(\beta^+\nu)^{25}$Mg$(p,\gamma)^{26}$Al. This production sequence can be by-passed by ^{25}Al$(p,\gamma)^{26}$Si$(p,\gamma)^{27}$P. It has been suggested [19] that higher temperature novae ($T_9 \approx 0.4$ GK) may be hot enough to establish an equilibrium between the isomeric state and the ground state of ^{26}Al. Thus, ^{26}Si destruction by proton capture is important for understanding this component of ^{26}Al(g.s.) production, as the isomeric level of ^{26}Al would not be fed by the ^{26}Si β decay. This component is expected to be small for lower-temperature burning scenarios, but may be significant at higher temperatures where equilibrium between ^{26m}Al and ^{26}Al(g.s.) is reached more quickly.

No experimental information are available about the two reaction rates. Present estimates are based on shell model predictions [13] which include both direct capture as well as resonant contributions. Inconsistencies exist in particular for the level structure of ^{27}P. While mirror-nucleus analysis predicts a 0.98 MeV state near the threshold [20], detailed shell model calculations indicate a shift towards higher energies predicting this state as the dominant resonance for the proton capture rate in ^{26}Si$(p,\gamma)^{27}$P. These calculations and lack of experimental evidence lead to more than three orders of magnitude uncertainty in the reaction rate [13]. Clearly, experimental verification of the predicted excitation energy is necessary to remove this uncertainty.

The reaction rates for proton capture processes on ^{22}Mg and ^{26}Si are dominated by direct capture transitions to the ground states and by resonant capture into isolated proton unbound states of the compound nuclei. The direct capture component of the reaction rate is determined by the nonresonant cross section $\sigma(E)$ of the transition. For charged particle interactions the cross section can be replaced by the astrophysical S factor [21]

$$S(E) = E \exp(2\pi\eta)\, \sigma(E) \tag{1}$$

with η denoting the Sommerfeld parameter. The S factor depends only weakly on the bombarding energy and the nonresonant reaction rate is given by

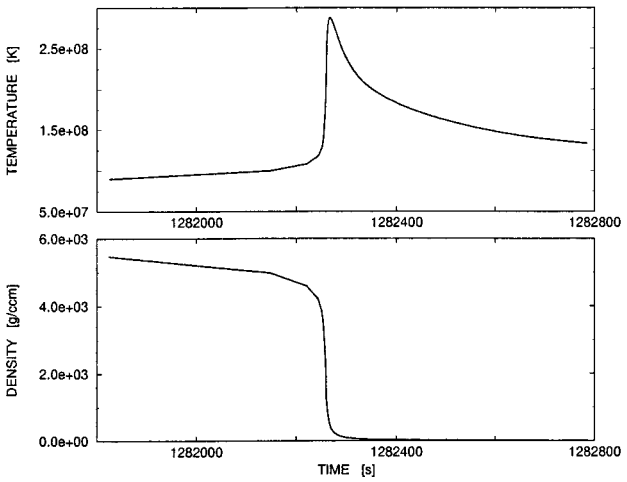

FIG. 1. Temperature and density conditions as predicted by nova models.

$$\langle \sigma \nu \rangle_{\rm dc} = 1.3 \times 10^{-14} \left(\frac{Z_1 Z_2}{A} \right)^{1/3} T_9^{-2/3} S_{\rm eff} \times \exp\left(-4.248 \frac{Z_1^2 Z_2^2 A}{T_9} \right)^{1/3}, \quad (2)$$

where the reduced mass A is given by $A_p A_T/(A_p+A_T)$ and A_p is the proton mass and A_T is the target mass, T_9 is the temperature in units [G K]. The effective S factor $S_{\rm eff}$ is in units [MeV b] is approximated by [22]

$$S_{\rm eff} = S_0 \left(1 - \frac{5 T_9^{1/3}}{50.976 (Z_1^2 2 Z_2^2 A)^{1/3}} \right). \quad (3)$$

Resonant capture rates for isolated, narrow resonances are given by

$$\langle \sigma \nu \rangle_{\rm res} = 2.557 \times 10^{-19} A^{-3/2} T_9^{-3/2} \omega\gamma \exp\left(\frac{-11.605 E_r}{T_9} \right). \quad (4)$$

The resonance strength $\omega\gamma$ (in units [eV]) is given by

$$\omega\gamma = \frac{2J+1}{(2J_p+1)(2J_T+1)} \frac{\Gamma_p \Gamma_\gamma}{\Gamma_{\rm tot}}, \quad (5)$$

where J is the spin of the compound nucleus and J_T is the spin of the target. Because of the exponential dependence on the resonance energy E_r (in units [MeV]), level energy uncertainties of 100 keV can produce orders of magnitude of uncertainty in the reaction rates. The proton width is normally determined by $\Gamma_p = C^2 S \Gamma_{\rm sp}$, where C^2S is the single particle spectroscopic factor and $\Gamma_{\rm sp}$ is the single particle width. The $\Gamma_{\rm sp}$ is determined by calculating phase shifts of the protons scattering off a Woods-Saxon potential whose depth is determined by matching the resonance energies [13]. The gamma decay widths Γ_γ are determined from the reduced electromagnetic transition probabilities and have an energy dependence specific to the type of transition. The total width $\Gamma_{\rm tot}$ is the sum of the partial widths.

A direct measurement of the relevant capture rate is the prefered method for determining the proton capture reaction rates. However, the cross sections become prohibitively small at stellar energies due to the repulsive Coulomb force, so other experimental methods must be employed to gain information about the levels. Radioactive beams of sufficient intensities are not yet available, so indirect spectroscopic measurements such as transfer reactions have been used to determine energy levels in proton rich nuclei. The (^{7}Li,^{8}He), (^{3}He,^{8}Li), and (^{4}He,^{8}He) reactions are examples of reactions that have been successfully used in the past for spectroscopic measurements of proton rich nuclei [14,17,23,24].

The ^{22}Mg$(p,\gamma)^{23}$Al reaction proceeds predominantly through resonant capture to the first excited state at nova temperatures. This state has only been observed once and was unresolved from the ground state [17]. The goal of this experiment was to take advantage of the high resolution and large acceptance of the S800 spectrograph to resolve the first excited state from the ground state and reduce the uncertainty in the excitation energy of the state to 20 keV or less. Another source of uncertainty is the proton separation energy of ^{23}Al [14]. Hence, a better mass measurement will improve the knowledge of this rate.

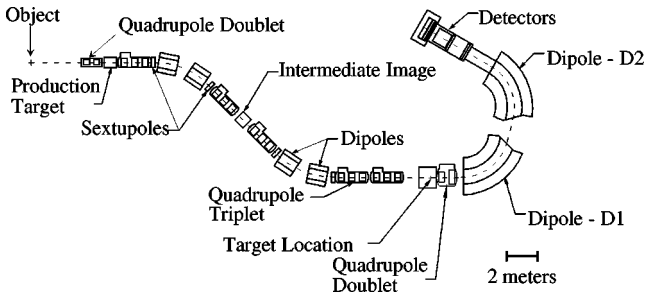

FIG. 2. The S800 spectrograph.

In the case of ^{27}P, there has been only one experimental report of excited states by Benenson *et al.* [24]. They observed one state at an excitation energy of 1.66(4), which lies too high above the proton threshold to be of any consequence in explosive hydrogen burning in nova. Evidence of a state at ≈ 1.2 MeV was present in the data of Benenson *et al.*, but was not conclusive and therefore was not reported. Another mass measurement of ^{27}P is also desirable since the first mass measurement is marginally consistent with the isobaric mass multiplet equation (IMME) prediction based on the other three members of the $T=3/2$ isospin quartet [23].

III. EXPERIMENT

The S800 magnetic spectrograph at MSU, shown in Fig. 2, has been described elsewhere [25,26]. The spectrograph was designed to have an energy resolving power of $E/\Delta E = 10\,000$, an angular resolution of $\leqslant 2$ mrad, and a 20 msr solid angle. It consists of a beam analysis line and the spectrograph itself. The beam analysis line is very similar to the A1200 fragment separator at MSU [27], but with larger acceptance and better resolution. The spectrograph consists of a large, superconducting quadrupole doublet followed by two 70-ton superconducting dipole magnets. The detectors in the focal plane consist of two position tracking detectors separated by approximately 1 m, an ionization chamber for energy loss measurements, and three thick plastic scintillators for total energy measurement [28] (see Fig. 2).

The spectrograph was operated in dispersion-matched mode to cancel the 0.08(1)% intrinsic beam energy spread. Ray-tracing techniques were used to reconstruct the energy of the ejectile from the target. The measured magnetic field data were used as input to an ion optics computer code COSY [29]. COSY calculates a transfer map from the target to the focal plane under the assumption that the beam spot is small, and the dispersion matching is perfect. The transfer map is then inverted, and with measurement of horizontal and vertical positions and angles in the focal plane, it is possible to deduce the energies, angles, and vertical positions of the emerging nuclei from the reaction in the target using the procedure described by Berz *et al.* [30].

The spectrograph was set for an angular coverage of $0-12°$ in the lab. A 50.1(3) MeV/nucleon ^{7}Li beam bom-

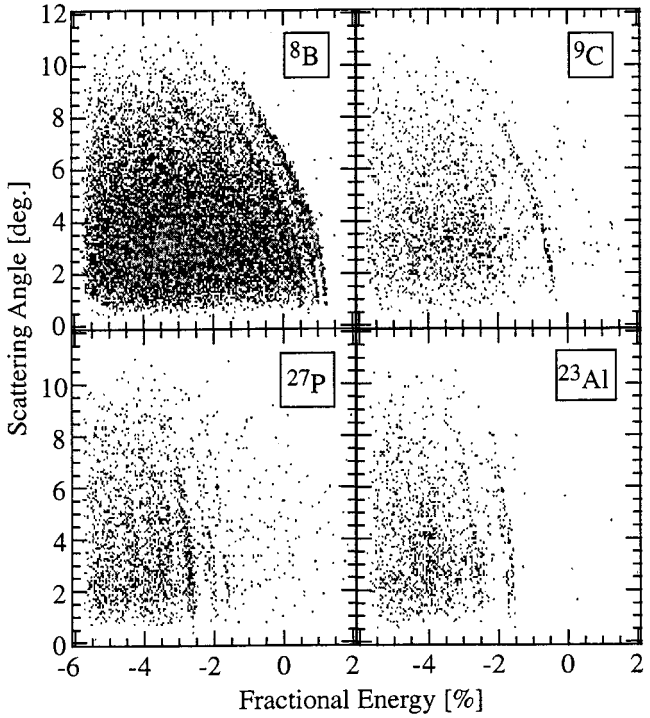

FIG. 3. Kinematic energy spectra of the four reactions, populating states in the listed nuclei.

barded four targets: 0.34(3) mg/cm^2 ^{10}B with a thin carbon backing, 0.94(9) mg/cm^2 ^{9}Be, 1.4(1) mg/cm^2 ^{nat}Si (we thank Virginia Semiconductor for providing the silicon wafer), and 0.63(6) mg/cm^2 ^{24}Mg (99.9% enriched). The ^{24}Mg(^{7}Li,^{8}He)^{23}Al and ^{28}Si(^{7}Li,^{8}He)^{27}P reactions were used to populate states in ^{23}Al and ^{27}P. The ^{10}B(^{7}Li,^{8}He)^{9}C and ^{9}Be(^{7}Li,^{8}He)^{8}B reactions were used for energy calibration.

The ^{8}He nuclei were unambiguously identified by energy loss measurements in an ion chamber and the tracking detectors, total energy measurements using a thick plastic scintillator, and time-of-flight measurements using the fast plastic scintillator signal with respect to the *rf* structure of the cyclotron. The two position tracking detectors were used to measure the positions and angles of the ^{8}He^{2+} ions reaching the focal plane. The total energy and scattering angle of the emerging ^{8}He were reconstructed using the aforementioned ray-tracing techniques.

Because of the extremely small cross sections ($\simeq 1-5$ nb/sr), scattered beam and its products posed a significant experimental challenge. The detectors could physically withstand the $\simeq 100$ kHz rate, but the data acquisition system could not. Programmable hardware gates were placed on the discriminated energy signals from the two photomultiplier tubes on the plastic scintillator which prevented the data acquisition system from generating a trigger unless the particles' energy signals fell within this gate. This trigger rejection scheme limited the event rate to $\simeq 1000$ Hz for beam currents up to 50 pnA, making the experiment possible.

IV. RESULTS

Figure 3 shows the reconstructed scattering angle plotted as a function of reconstructed energy for all four reactions used in this experiment. The energy is given in units of percent deviation from the central ray; the lines in the spectra have the expected kinematic shape. After reconstructing the scattering angle, the kinematics of the reactions were used to shift the energy of each event to what it would be at zero degrees. This procedure places all events corresponding to the same reaction Q value in the same peak and allows full utilization of the S800's 20 msr acceptance.

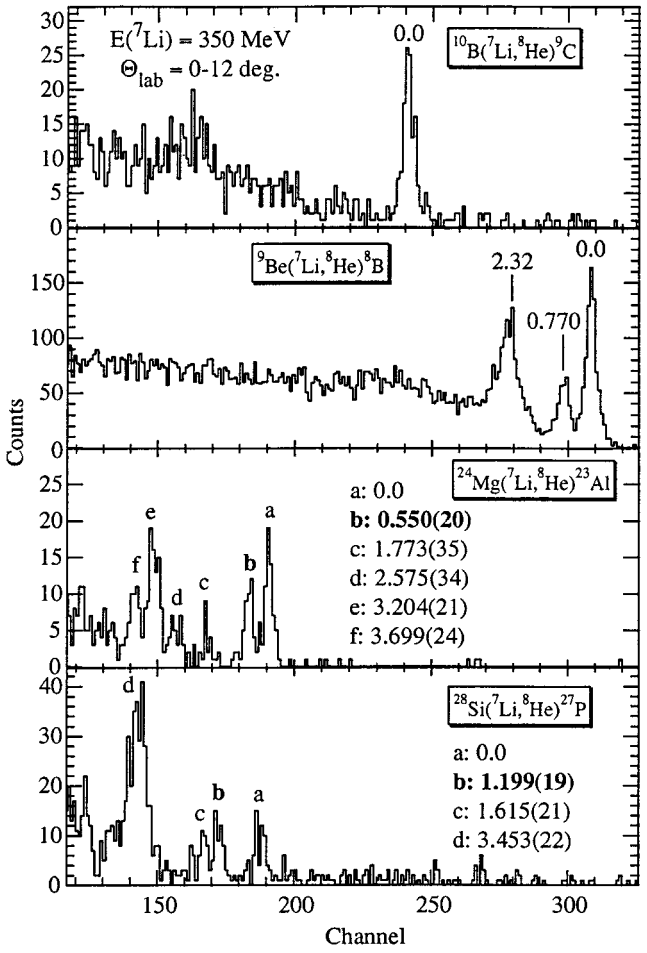

FIG. 4. Energy spectra of the four reactions. The states important in the *rp* process are listed in boldface type. The first excited state in ^{23}Al is resolved from the ground state for the first time at 0.550(20) MeV. The first excited state of ^{27}P is measured for the first time at 1.199(19) MeV.

TABLE I. Experimental observations of states in ^{23}Al.

ME [MeV]	E_x [MeV]	Previously measured ME [MeV]	Avg. [MeV]
6.773(28)	0.00	6.767(25) [23]	6.770(19)
7.322(30)	0.550(20)	7.23(6) [17]	E_x=0.528(19)
8.545(44)	1.773(35)		
9.348(42)	2.575(34)		
9.95(33)	3.204(21)		
10.47(36)	3.699(24)		

TABLE II. Experimental observations of states in ^{27}P.

ME [MeV]	E_x [MeV]	Previously measured ME [MeV]	Avg. [MeV]
-0.670(41)	0.00	-0.753(35) [24]	-0.715(27)
0.529(42)	1.199(19)		
0.945(44)	1.615(21)	0.91(4) [24]	E_x=1.631(19)
2.783(46)	3.453(22)		

Figure 4 shows all the energy spectra created in this manner which were accumulated throughout the experiment. The peak shapes expected from simulations using the reaction kinematics and primary beam angular divergence ($\simeq$5 mrad) were well approximated by Lorentzians that were consequently used to fit the observed peaks. The resulting fits matched the observed peaks for all reactions well. The ground state of ^{9}C ($Q_0=-33.5534$ MeV [31]) and the ground and first excited states of ^{8}B ($Q_0=-28.2636$ MeV [31]) were used to establish the energy calibration. The energy resolution was limited by the primary beam angular divergence for the ^{9}Be(^{7}Li,^{8}He)^{8}B and ^{10}B(^{7}Li,^{8}He)^{9}C reactions, and by the target thickness for the ^{24}Mg(^{7}Li,^{8}He)^{23}Al and ^{28}Si(^{7}Li,^{8}He)^{27}P reactions. The best energy resolution achieved was 1 part in 1700 for the ^{24}Mg(^{7}Li,^{8}He)^{23}Al reaction.

Tables I and II list the mass excesses (MEs) of each state, the excited state locations with respect to the observed ground state, previous measurements (when existing) and weighted averages of the past and present measurements for peaks in the ^{23}Al and ^{27}P energy spectra. The quoted uncertainties include systematic and statistical contributions. The uncertainties on the mass excesses are dominated by the scattering angle uncertainty of $\pm 0.05°$; the excited state uncertainties are purely statistical.

V. DISCUSSION

A. Mass measurements and the IMME

The ground state mass measurements made here are of the same quality as existing mass measurements for the two nuclei. The mass uncertainties in ^{23}Al and ^{27}P are thereby reduced due to these measurements. When combined with the preceding measurements, the mass excesses are 6.770(19) MeV and $-715(27)$ keV for ^{23}Al and ^{27}P, respectively.

TABLE III. The spectroscopic factors of the final states in ^{23}Al and ^{27}P and the resulting S factor for the direct capture to these states.

Reaction	E_x [MeV]	J^π	l_i	nl_f	C^2S	S_0 [MeV b]
^{22}Mg(p,γ)^{23}Al	0.0	$5/2^+$	p	$1d_{5/2}$	0.34 [17]	6.63×10^{-4}
			f	$1d_{5/2}$	0.34 [17]	6.90×10^{-5}
^{26}Si(p,γ)^{27}P	0.0	$1/2^+$	p	$2s_{1/2}$	0.46 [13]	3.63×10^{-2}

These weighted averages agree with the IMME predictions based on the other three members of the $T=3/2$ quartets; these nuclei are the $T_z=-3/2$ members of their respective isospin quartets.

The measurement of the first excited state of ^{27}P at 1.199 MeV provides the $T_z=-3/2$ point for the $T=3/2$, $J^\pi=3/2^+$ isospin quartet. Since the ^{27}Si member has not been identified, this measurement can provide a fairly accurate prediction for its location. Using the IMME coefficients obtained by fitting the three existing measurements of mass excesses [32] with a quadratic function and evaluating the function at $T_z=-1/2$, a prediction of $E_x=7741.5(74)$ keV for ^{27}Si can be made. A level has been observed at $E_x=7740.8(9)$ MeV in ^{27}Si but is assigned $9/2^+$ or $11/2^+$ [32]. Five other levels exist within 100 keV of this prediction but none have spin-parity assignments. A search for this level, perhaps with a light ion transfer reaction, would be desirable.

B. Implications for the stellar reaction rates

Figure 5 shows the updated capture reaction rates along with previously known information. The reaction rates for ^{22}Mg(p,γ)^{23}Al and ^{26}Si(p,γ)^{27}P are determined by a strong direct capture component [see Eq. (2)] and by resonant capture into the first excited state of the respective compound nucleus [see Eq. (4)]. The direct capture cross section itself has been calculated from the overlap of the free particle scattering wave function in the entrance channel, the bound state wave function in the exit channel and the dominant $E1$ electromagnetic transition operator in its long range approximation [33]. The wave functions were derived in the framework of a Woods-Saxon potential model [34]. The spectroscopic factor of the final state have been adopted from previous

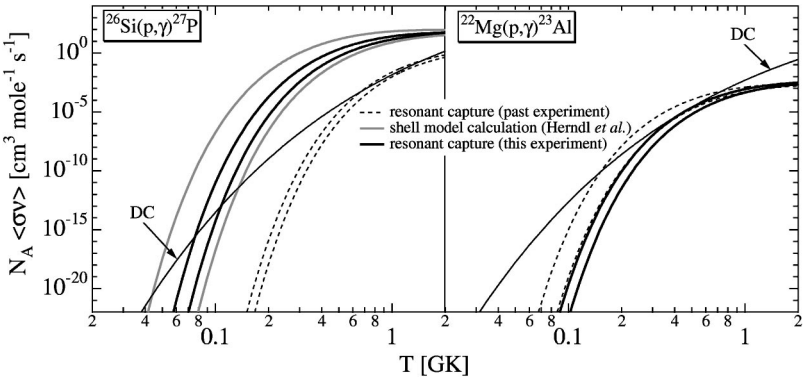

FIG. 5. Revised reaction rates for the two listed proton capture reactions using data obtained in this experiment. ''DC'' is the direct capture contribution to the rate. The pairs of lines are the upper and lower limits of the rates due to the 1σ uncertainties in the resonance locations. The gray solid lines in the left panel represent the resonant rate into the first excited state of ^{27}P as predicted by Herndl *et al.* The experimental result for the first excited state of ^{27}P is consistent with this shell model prediction, but has a much smaller uncertainty.

TABLE IV. The resonance parameters of proton unbound states in ^{23}Al and ^{27}P.

Reaction	E_x [MeV]	E_r [MeV]	J^π	Γ_γ [eV]	C^2S	Γ_p [eV]	$\omega\gamma$ [eV]
^{22}Mg$(p,\gamma)^{23}$Al	0.528	0.405(27)	$1/2^+$	5.49×10^{-7}	0.66 [17]	74.0	5.5×10^{-7}
^{26}Si$(p,\gamma)^{27}$P	1.199	0.340(33)	$3/2^+$	3.43×10^{-3}	0.41 [13]	3.5×10^{-3}	3.5×10^{-3}
	1.631	0.772(33)	$5/2^+$	3.30×10^{-4}	0.13 [13]	7.5	9.9×10^{-4}

shell model calculations [13,17]. The spectroscopic parameters for the calculation are listed in Table III.

For ^{22}Mg$(p,\gamma)^{23}$Al the direct capture is dominated by the $p\rightarrow d$ transition to the ground state in ^{23}Al. In Ref. [17] by mistake a dominant $f\rightarrow d$ transition has been quoted which is only a $\approx$10% component of the total cross section. This correction results in a significantly stronger direct capture component than previously claimed [17]. The S factor S_0 shown in Table III represents the averaged value of the calculated $S(E)$ over the characteristic energy range of novae burning, i.e., 0.1 to 0.3 MeV. For ^{26}Si$(p,\gamma)^{27}$P the direct capture is dominated by the $p\rightarrow d$ transition to the ground state in ^{27}P. The transition has been discussed in detail before; the previously predicted S-factor values have been adopted and are shown in Table III [13].

The resonant component of the reaction rates for ^{22}Mg$(p,\gamma)^{23}$Al and ^{26}Si$(p,\gamma)^{27}$P have been calculated using Eq. (4). The resonance energies E_r have been derived from the newly measured excitation energies and the here derived Q values of the reactions, $E_r=E_x-Q$. The Q value for ^{22}Mg$(p,\gamma)^{23}$Al has changed slightly based on the present data to $Q=0.123$ MeV. The new experimental results however also indicate a significant shift in resonance energy for ^{22}Mg$(p,\gamma)^{23}$Al. This reduces the resonant contribution to the reaction rate significantly within the temperature range of nova burning. For ^{26}Si$(p,\gamma)^{27}$P the experimental results confirmed the shell model prediction of a resonance state above the proton threshold. This observation therefore removed the biggest uncertainty for the determination of the reaction rate. The resonance strengths $\omega\gamma$ have been calculated from the proton and γ widths of the experimentally observed first excited states using Eq. (5). For ^{22}Mg$(p,\gamma)^{23}$Al the resonance strength is roughly a factor of 2 higher than before [17] due to the higher excitation energy of the resonance state. For ^{26}Si$(p,\gamma)^{27}$P the Q value is $Q=0.859$ MeV, which is a weighted average of this mass measurement and that of Benenson *et al.* [24], and is the same Q-value used in Herndl *et al.* [13]. The observed excitation energy for the first excited state is higher by $\approx$20 keV than the shell model prediction, which increases the resonance strength slightly beyond the previous predictions [13]. The resonance parameters for both reactions are listed in Table IV. The uncertainties in the resonance energies are quadrature sums of the target mass, the final mass, and the excitation energy.

The direct capture and the resonant reactions rate contributions for ^{22}Mg$(p,\gamma)^{23}$Al and ^{26}Si$(p,\gamma)^{27}$P are listed in Tables V and VI, respectively. For comparison also shown are the previously predicted rates based on the known shell model structure of the compound nuclei [17,13] and on statistical Hauser-Feshbach predictions which has been calculated using the code NON-SMOKER [35]. While in the case of ^{22}Mg$(p,\gamma)^{23}$Al the previous direct capture and resonant components differ considerably from the present results, the overall rate remains essentially unchanged since the increase of direct capture cross section is compensated by the decrease of resonance contribution to the rate. The comparison with the NON-SMOKER prediction shows that the Hauser Feshbach rate is substantially larger than the present rate due to

TABLE V. The reaction rate of ^{22}Mg$(p,\gamma)^{23}$Al in units [cm^3/mole/s] as a function of temperature. Listed are the direct capture and the resonance contribution. Also listed are the total rate and the previous estimate based on the level structure of the compound nucleus and statistical model predictions based on the code NON-SMOKER.

T [G K]	$N_A\langle\sigma v\rangle_{\rm dc}$	$N_A\langle\sigma v\rangle_{\rm res}$	$N_A\langle\sigma v\rangle_{\rm tot}$	$N_A\langle\sigma v\rangle_{\rm prev}$ [17]	$N_A\langle\sigma v\rangle_{HF}$ [35]
0.10	1.70×10^{-13}	1.32×10^{-21}	1.70×10^{-13}	1.70×10^{-13}	1.18×10^{-8}
0.15	5.13×10^{-11}	9.20×10^{-15}	5.13×10^{-11}	5.35×10^{-11}	2.18×10^{-6}
0.20	1.87×10^{-9}	2.14×10^{-11}	1.89×10^{-9}	2.92×10^{-9}	3.95×10^{-5}
0.30	1.66×10^{-7}	4.16×10^{-8}	2.08×10^{-7}	5.99×10^{-7}	1.13×10^{-3}
0.40	2.81×10^{-6}	1.61×10^{-6}	4.42×10^{-6}	1.06×10^{-5}	8.34×10^{-3}
0.50	2.09×10^{-5}	1.34×10^{-5}	3.43×10^{-5}	6.15×10^{-5}	3.29×10^{-2}
0.60	9.62×10^{-5}	5.25×10^{-5}	1.49×10^{-4}	2.12×10^{-4}	9.09×10^{-2}
0.70	3.24×10^{-4}	1.34×10^{-4}	4.58×10^{-4}	5.62×10^{-4}	2.00×10^{-1}
0.80	8.77×10^{-4}	2.64×10^{-4}	1.14×10^{-3}	1.27×10^{-3}	3.75×10^{-1}
0.90	2.04×10^{-3}	4.37×10^{-4}	2.48×10^{-3}	2.62×10^{-3}	6.29×10^{-1}
1.00	4.21×10^{-3}	6.44×10^{-4}	4.86×10^{-3}	4.98×10^{-3}	9.70×10^{-1}
1.50	5.23×10^{-2}	1.80×10^{-3}	5.41×10^{-2}	5.38×10^{-2}	4.02×10^{0}
2.00	2.52×10^{-1}	2.65×10^{-3}	2.54×10^{-1}	2.54×10^{-1}	9.04×10^{0}

TABLE VI. The reaction rate of ^{26}Si$(p,\gamma)^{27}$P in units [cm^3/mole/s] as a function of temperature. Listed are the direct capture and the resonance contribution. Also listed are the total rate and the previous estimate based on the level structure of the compound nucleus and statistical model predictions based on the code NON-SMOKER.

T [G K]	$N_A\langle\sigma v\rangle_{\rm dc}$	$N_A\langle\sigma v\rangle_{\rm res}$	$N_A\langle\sigma v\rangle_{\rm tot}$	$N_A\langle\sigma v\rangle_{\rm prev}$ [13]	$N_A\langle\sigma v\rangle_{\rm HF}$ [35]
0.10	3.89×10^{-14}	2.28×10^{-13}	2.67×10^{-13}	6.19×10^{-13}	2.50×10^{-9}
0.15	2.37×10^{-11}	6.38×10^{-8}	6.38×10^{-8}	7.50×10^{-8}	1.99×10^{-6}
0.20	1.33×10^{-9}	2.98×10^{-5}	2.98×10^{-5}	2.37×10^{-5}	7.50×10^{-5}
0.30	2.03×10^{-7}	1.16×10^{-2}	1.16×10^{-2}	6.30×10^{-3}	4.28×10^{-3}
0.40	4.74×10^{-6}	2.02×10^{-1}	2.02×10^{-1}	9.04×10^{-2}	4.29×10^{-2}
0.50	4.43×10^{-5}	1.04×10^{0}	1.04×10^{0}	4.14×10^{-1}	1.97×10^{-1}
0.60	2.44×10^{-4}	2.95×10^{0}	2.95×10^{0}	1.09×10^{0}	5.92×10^{-1}
0.70	9.41×10^{-4}	5.99×10^{0}	5.99×10^{0}	2.09×10^{0}	1.36×10^{0}
0.80	2.88×10^{-3}	9.92×10^{0}	9.92×10^{0}	3.32×10^{0}	2.62×10^{0}
0.90	7.39×10^{-3}	1.44×10^{1}	1.44×10^{1}	4.67×10^{0}	4.45×10^{0}
1.00	1.64×10^{-2}	1.90×10^{1}	1.90×10^{1}	6.04×10^{0}	6.88×10^{0}
1.50	2.80×10^{-1}	3.88×10^{1}	3.90×10^{1}	1.17×10^{1}	2.76×10^{1}
2.00	1.65×10^{0}	4.89×10^{1}	5.06×10^{1}	1.57×10^{1}	5.88×10^{1}

the low level density at low excitation energies of the compound nucleus ^{23}Al. Resonant contributions of the higher excited states at 1.773 and 2.575 MeV may contribute to the reaction rates at temperatures $T \geqslant 2$ G K and are therefore negligible for nova conditions. (For higher temperatures these resonances account for at most 10% of the total rate.) For temperatures above 2 G K the Hauser Feshbach rate should be adopted. For the case of ^{26}Si$(p,\gamma)^{27}$P the present rate is in reasonably good agreement with the previous shell model based estimates. The deviation is due to the slight difference between the shell model based prediction for the excitation energy [13] and the actual experimental result. The Hauser Feshbach prediction agrees within a factor of 6 with the rate presented here. That is mainly due to the strong direct capture component because of the relatively low level density in the compound nucleus ^{27}P.

To investigate the consequences of the new reaction rates for the nucleosynthesis of the long-lived γ emitters ^{22}Na and ^{26}Al reaction network calculations have been performed in post-processing mode within the framework of a simplified model for Ne novae [2]. The temperature curve for the inner mass zone is displayed in Fig. 1. Figure 6 shows the associated reaction flow in the Ne-Si mass range integrated over the entire time period of the thermonuclear runaway. The reaction flow is characterized by the hot NeNa and the MgAl cycles processing the long-lived γ emitters ^{22}Na and ^{26}Al. It can clearly be seen that the main reaction flow processes ^{22}Mg by β decay towards ^{22}Na. Because of its low Q value the ^{22}Mg$(p,\gamma)^{23}$Al reaction is in equilibrium with its inverse reaction ^{23}Al$(\gamma,p)^{22}$Mg. Figure 7 shows the corresponding

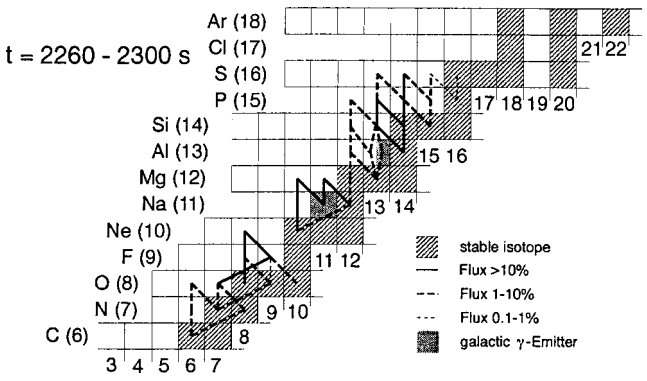

FIG. 6. Reaction flow integrated over the time period of the thermonuclear runaway as simulated in the framework of a one-zone nova model.

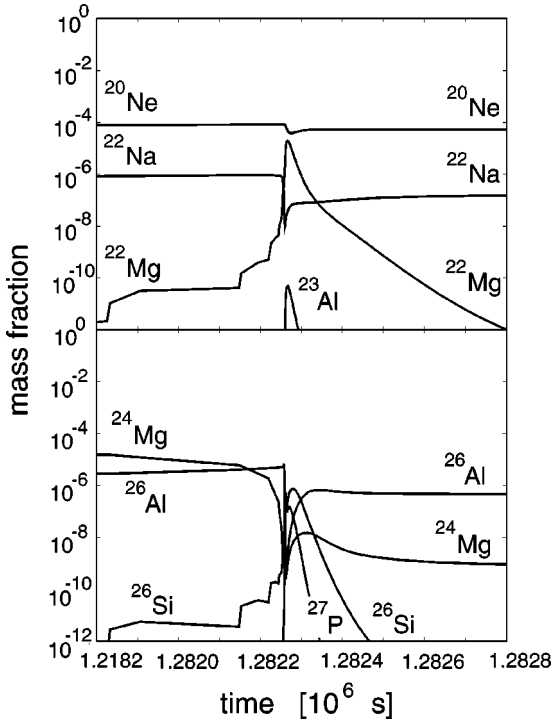

FIG. 7. Nuclear abundances before, during, and after a nova outburst. See text for details.

abundance development for ^{22}Mg, ^{22}Na, as well as for ^{26}Si, ^{26}Al. Also shown for comparison are the abundances for the stable feeding nuclei ^{20}Ne and ^{24}Mg. Figure 7 shows that there is only a minute change of the abundance of ^{20}Ne through the burst, due to the very small reaction rate for ^{20}Ne$(p,\gamma)^{21}$Na [36]. The resulting abundance for ^{22}Na is therefore relatively small. The burst of ^{22}Mg production during the thermonuclear runaway compensates for the parallel loss of ^{22}Na through proton capture but only limited production of ^{23}Al/^{24}Si is observed. Comparison between the present and the previous rates only showed insignificant differences. This is due to the fact that the peak temperature of the nova burst is appreciably below the temperature where such changes have been anticipated [14]. In the case of ^{24}Mg a rapid depletion is observed during the thermonuclear runaway due to the strong ^{24}Mg$(p,\gamma)^{25}$Al rate [37]. This converts rapidly into ^{26}Al through ^{25}Al$(\beta^+\nu)^{25}$Mg$(p,\gamma)^{26}$Al. The branch through ^{25}Al$(p,\gamma)^{26}$Si does not contribute to the ground state formation of ^{26}Al since it either bypasses ^{26}Al altogether through the ^{26}Si$(p,\gamma)^{27}$P reaction or feeds the isomeric 0^+ state in ^{26}Al which decays predominantly by β decay to ^{26}Mg [38,19]. The feeding of the ground state of ^{26}Al in novae therefore depends entirely on the ^{25}Al$(\beta^+\nu)$-^{25}Al(p,γ) branching ratio. The ^{26}Al abundance produced in novae also depends on the initial abundance of ^{24}Mg which originates from O,Ne white dwarf material mixed into the burning zone by convective or shear processes [39]. Recent predictions [40] of stellar abundance distributions for stars after their carbon burning phase predicted a significantly smaller ^{24}Mg abundance than previously assumed [41], which has been shown to have significant consequences for the ^{26}Al production during the Nova thermonuclear runaway [6]. More detailed studies with regard to the white dwarf material and also with regard to the nature of the mixing processes will be extremely important for a reliable prediction of ^{22}Na and ^{26}Al production in novae.

VI. CONCLUSIONS

Using the S800 spectrograph at MSU, the nuclei ^{23}Al and ^{27}P were studied using the (^{7}Li,^{8}He) reaction. Ground state masses and first excited states in these nuclei, which are relevant to the production of cosmic γ-ray emitters ^{22}Na and ^{26}Al, have been measured. The ground state mass excesses of ^{23}Al and ^{27}P were measured to be 6.773(28) and $-0.670(41)$, respectively. These measurements are consistent with past measurements and the IMME predictions based on isobaric analog states. The first excited state in ^{23}Al was resolved from the ground state for the first time at $E_x = 550(20)$ keV. This measurement has a negligible effect on the reaction rates, but reduces the uncertainty in reaction rates and hence the production of ^{22}Na in novae. The first excited state in ^{27}P was measured at $E_x = 1.199(19)$ MeV. This measurement greatly reduces the uncertainty of the properties of this state which was only known by a shell model calculation and never before reported experimentally. While these measurements do not significantly change the reaction rates, they greatly reduce the uncertainties in the reaction rates which is very important in determining where the largest remaining uncertainties lie and which reactions should be investigated in the future.

ACKNOWLEDGMENTS

This work was supported by the U.S. National Science Foundation under Grant No. PHY9528844 and by the U.S. Department of Energy, Nuclear Physics Division, under Contract No. W-31-109-ENG-38.

[1] R.D. Gehrz, J.W. Truran, R.E. Williams, and S. Starrfield, Publ. Astron. Soc. Pac. **110**, 3 (1998).
[2] S. Starrfield, J.W. Truran, M. Wiescher, and W.M. Sparks, Mon. Not. R. Astron. Soc. **296**, 502 (1998).
[3] R.D. Gehrz, G.L. Grasdalen, and J.A. Hackwell, Astrophys. J. Lett. **298**, L47 (1985).
[4] A.E. Champagne and M. Wiescher, Annu. Rev. Nucl. Part. Sci. **42**, 39 (1992).
[5] E.M. Sion, F.H. Cheng, W.M. Sparks, P. Szkody, M. Huang, and I. Hubeny, Astrophys. J. Lett. **480**, L17 (1997).
[6] J. Jose, A. Coc, and M. Hernanz, Astrophys. J. **520**, 347 (1999).
[7] S. Wanajo, M. Hashimoto, and K. Nomoto, Astrophys. J. **523**, 409 (1999).
[8] S. A. Glasner, E. Livne, and J.W. Truran, Astrophys. J. **475**, 754 (1997).
[9] A. Kercek, W. Hillebrandt, and J.W. Truran, Astron. Astrophys. **337**, 379 (1998).
[10] P. Haustein, S. Starrfield, S.N. Shore, F. Allard, and E. Baron, Astrophys. J. **447**, 829 (1995).
[11] I. Iyudin *et al.*, Astron. Astrophys. **300**, 422 (1995).
[12] L. VanWormer, J. Görres, C. Iliadis, M. Wiescher, and F.-K. Thielemann, Astrophys. J. **432**, 326 (1994).
[13] H. Herndl, J. Görres, M. Wiescher, B.A. Brown, and L. Van Wormer, Phys. Rev. C **52**, 1078 (1995).
[14] H. Schatz *et al.*, Phys. Rev. Lett. **79**, 3845 (1997).
[15] S. Schmidt, C. Rolfs, W.H. Schulte, H.P. Trautvetter, R.W. Kavanagh, C. Hategan, S. Faber, B.D. Valnion, and G. Graw, Nucl. Phys. **A591**, 227 (1995).
[16] F. Stegmüller, C. Rolfs, S. Schmidt, W.H. Schulte, H.P. Trautvetter, and R.W. Kavanagh, Nucl. Phys. **A601**, 168 (1996).
[17] M. Wiescher, J. Görres, B. Sherrill, M. Mohar, J.S. Winfield, and B.A. Brown, Nucl. Phys. **A484**, 90 (1988).
[18] N. Prantzos, R. Diehl, Phys. Rep. **267**, 1 (1995).
[19] A. Coc, M.-G. Porquet, and F. Nowacki, Phys. Rev. C **61**, 015801 (1999).
[20] M. Wiescher, J. Görres, F.-K. Thielemann, and H. Ritter, Astron. Astrophys. **160**, 56 (1986).
[21] W.A. Fowler, G.R. Caughlan, and B.A. Zimmerman, Annu. Rev. Astron. Astrophys. **5**, 525 (1967).
[22] W.A. Fowler, G.R. Caughlan, and B.A. Zimmerman, Annu. Rev. Astron. Astrophys. **13**, 69 (1975).

[23] W. Benenson, G. Guichard, E. Kashy, D. Mueller, H. Nann, and L.W. Robinson, Phys. Lett. **58B**, 46 (1975).
[24] W. Benenson, D. Mueller, E. Kashy, H. Nann, and L.W. Robinson, Phys. Rev. C **15**, 1187 (1977).
[25] J.A. Caggiano, Ph.D. thesis, Michigan State University, 1999.
[26] J.A. Nolen, Jr. *et al.*, MSU-NSCL Report No. MSU-694, 1989.
[27] B.M. Sherrill, D.J. Morrissey, J.A. Nolen, Jr., N. Orr, and J.A. Winger, Nucl. Instrum. Methods Phys. Res. B **70**, 298 (1992).
[28] J. Yurkon, D. Bazin, W. Benenson, D.J. Morrissey, B.M. Sherrill, D. Swan, and R. Swanson, Nucl. Instrum. Methods Phys. Res. A **422**, 291 (1999).
[29] M. Berz, Nucl. Instrum. Methods Phys. Res. A **298**, 473 (1992).
[30] M. Berz, K. Joh, J.A. Nolen, B.M. Sherrill, and A.F. Zeller, Phys. Rev. C **47**, 537 (1993).
[31] G. Audi and A.H. Wapstra, Nucl. Phys. **A565**, 1 (1993).
[32] P.M. Endt, Nucl. Phys. **A521**, 1 (1990).
[33] G.M. Bailey, G.M. Griffith, and T.W. Donelly, Nucl. Phys. **A94**, 502 (1967).
[34] C. Iliadis, L. Buchmann, P.M. Endt, H. Herndl, and M. Wiescher, Phys. Rev. C **53**, 475 (1996).
[35] T. Rauscher, F.-K. Thielemann, and K.L. Kratz, Phys. Rev. C **56**, 1613 (1997).
[36] C. Angulo *et al.*, The NACRE Collaboration, Nucl. Phys. **A656**, 3 (1999).
[37] D.C. Powell, C. Iliadis, A.E. Champagne, C.A. Grossmann, S.E. Hale, V.Y. Hansper, and L.K. McLean, Nucl. Phys. **A660**, 349 (1999).
[38] R.A. Ward, and W.A. Fowler, Astrophys. J. **238**, 266 (1980).
[39] A. Weiss and J.W. Truran, Astron. Astrophys. **238**, 178 (1990).
[40] C. Ritossa, E. Garcia-Berro, and I. Iben, Astrophys. J. **460**, 489 (1996).
[41] D. Arnett and J.W. Truran, Astrophys. J. **157**, 339 (1969).